A combined stopped-flow, electrospray ionization mass spectrometry and ^{31}P NMR study on the acetic acid-mediated fragmentation of the hydroxo-chalcogenide cluster $[W_3Se_4(OH)_3(dmpe)_3]^+$ (dmpe = 1,2-bis(dimethylphosphanyl)ethane) to yield the dinuclear $[W_2Se_2(\mu\text{-}Se)_2(\mu\text{-}CH_3CO_2)(dmpe)_2]^+$ complex†

Andrés G. Algarra,[a] Manuel G. Basallote,*[a] C. Esther Castillo,[a] Carolina Corao,[b] Rosa Llusar,*[b] M. Jesús Fernández-Trujillo[a] and Cristian Vicent[b]

Received 4th August 2006, Accepted 25th September 2006
First published as an Advance Article on the web 11th October 2006
DOI: 10.1039/b611274a

The reaction of the incomplete-cuboidal $[W_3Se_4(OH)_3(dmpe)_3]^+$ ([**1**]$^+$) cluster with acetic acid in acetonitrile solution leads to cluster fragmentation with formation of the dinuclear $[W_2Se_2(\mu\text{-}Se)_2(\mu\text{-}CH_3CO_2)(dmpe)_2]^+$ ([**2**]$^+$) complex. The X-ray structure of [**2**]PF_6 presents two equivalent metal centres bridged by one acetate ligand. Each W atom is additionally coordinated by one terminal selenium atom, two bridging selenido and two diphosphane phosphorus atoms in an essentially octahedral environment. Stopped-flow and conventional UV-vis studies indicate that fragmentation of [**1**]$^+$ into [**2**]$^+$ occurs through a complex mechanism. Three steps can be distinguished in the stopped-flow time scale, all of them showing a first order dependence with respect to the acetic acid concentration, followed by very slow spectral changes that lead to the formation of [**2**]$^+$. Phosphorus NMR, electrospray ionization mass spectrometry (ESI-MS) and tandem mass spectrometry (ESI-MS/MS) have been used to identify the nature of the reaction intermediates formed in the different steps. These studies indicate that the first two steps correspond to the formal substitutions of the hydroxo ligands at two metal centres by terminal acetate ligands. The third step involves bridging of one of the terminal acetate ligands, which actually prepares the trinuclear cluster to afford the acetate-bridged $[W_2Se_2(\mu\text{-}Se)_2(\mu\text{-}CH_3CO_2)(dmpe)_2]^+$ ([**2**]$^+$) complex. Although the precise details of the final conversion to [**2**]$^+$ have not been established, the results obtained by combination of the different experimental techniques provide a complete picture of the speciation of the cluster [**1**]$^+$ in acetonitrile solutions containing acetic acid.

1 Introduction

Organometallic compounds with terminal hydroxo ligands play an important role in many biological systems and have been proposed as intermediates in numerous catalytic processes.[1–4] Studies on the reactivity of this kind of compounds have been long hindered due to the synthetic difficulties associated to their preparation and isolation,[5] which mainly arise from their strong tendency to form polynuclear hydroxo-bridged species.[6] From a synthetic point of view, it is well-known that the presence of bulky ligands at the proximities of the metal site prevents the formation of OH^--bridged species. Besides this requirement, most synthetic procedures rely on the presence of adventious water in the reaction mixture or the reaction with KOH in dry tetrahydrofuran, CH_2Cl_2/water or molten KOH as hydroxo synthons.[5,7,8]

In particular, group VI hydroxo complexes are typically found as polynuclear entities with doubly and triply-bridging hydroxo ligands.[6] Examples of mononuclear group VI complexes with terminal hydroxo ligands are less common,[7,9–11] and their polynuclear homologues are even more scarce, despite the fact that the latter class of compounds can be used as molecular models to study reactions of metal oxides surfaces with small molecules. In this sense, O'Hair and co-workers have taken advantage of the easy preparation and isolation of the $[M_2O_6(OH)]^-$ ions (M = Mo, W) in tandem mass spectrometers to study their gas-phase reactivity with alcohols. The dinuclear terminal hydroxo $[Mo_2O_6(OH)]^-$ complex has proved to be efficient gas-phase catalysts in the formation of aldehydes while its mononuclear $[MoO_3(OH)]^-$ congener is inert. These results suggest that $[Mo_2O_6(OH)]^-$ ion is a good candidate to model molybdenum oxide surfaces active sites.[12,13] Analogous gas-phase studies reveal that acetic acid can be efficiently converted to ketene mediated by $[M_2O_6(OH)]^-$ ions (M = Mo, W) and a parallelism between gas-phase *vs.* surface metal oxide is also drawn.[14] Although these results provide fundamental information on the elementary steps in the gas-phase catalytic cycle, we are far from understanding the speciation chemistry in solution of polynuclear systems with terminal hydroxo ligands. The speciation chemistry of a closely related compound,

[a]*Departamento de Ciencia de los Materiales e Ingeniería Metalúrgica y Química Inorgánica, Facultad de Ciencias, Universidad de Cádiz, Apartado 40, Puerto Real, 11510, Cádiz, Spain*
[b]*Departament de Ciències Experimentals, Universitat Jaume I, Campus de Riu Sec, Box 224, 12071, Castelló, Spain; Fax: +34 964 728066; Tel: +34 964 728086*

† Electronic supplementary information (ESI) available: ESI-MS/MS of species generated from [**1**]$^+$, [**I$_1$**]$^+$, [**I$_2$**]$^+$ and [**2**]$^+$. See DOI: 10.1039/b611274a

namely $[(C_5Me_5)Mo_2O_5]$ has been extensively studied in water–methanol mixtures,[15–17] and although the presence of terminal hydroxo intermediates has been proposed, its transient nature precludes a detailed reactivity study.

From the comments above, it is evident that any knowledge regarding solution speciation chemistry of group VI polynuclear complexes with terminal OH^- ligands is critical to envision new applications. This point of view might represent an alternative to the modelling of group VI oxide surfaces and beyond all doubt it will also contribute to the better understanding of the fundamental chemical properties of the M–OH bonds.

Recently, our group has reported the synthesis of the terminal hydroxo complex of general formula $[W_3Se_4(OH)_3(dmpe)_3]^+$ ($[\mathbf{1}]^+$) starting from the bromine or hydride analogues in the presence of sodium hydroxide solutions in water–acetonitrile mixtures or acetonitrile solutions with traces of water, respectively.[18] Each cluster unit contains one hydroxo ligand coordinated to a tungsten site in a overall C_3 symmetry (see Scheme 1). Mechanistic studies on the reaction of this complex with HX acids (X = Cl, Br) in acetonitrile-water solutions revealed that OH^--protonation gives rise to $[W_3Se_4(OH_2)_3(dmpe)_3]^{4+}$ followed by substitution of the aqua ligands by X^- to afford $[W_3Se_4X_3(dmpe)_3]^+$. To extend our research on the behaviour of these complexes, we report herein a study of the reactivity of the trihydroxo $[W_3Se_4(OH)_3(dmpe)_3]PF_6$ complex in CH_3CO_2H–CH_3CN media. Despite the fact that we have no evidence of catalytic transformation of acetic acid in the presence of complex $[\mathbf{1}]^+$, this acid reacts with $[\mathbf{1}]^+$ in a different way to that found for hydrogen halides to produce an acetate-bridged dinuclear $[W_2Se_2(\mu\text{-}Se)_2(\mu\text{-}CH_3CO_2)(dmpe)_2]^+$ ($[\mathbf{2}]^+$) cluster. The detailed mechanistic study on the reaction of $[\mathbf{1}]^+$ with acetic acid in acetonitrile solution has been elucidated through a combined stopped-flow, ^{31}P NMR, electrospray ionization mass spectrometry (ESI-MS) and tandem mass spectrometry (ESI-MS/MS) study. Whereas the benefits of using NMR spectroscopy for monitoring reactions of these clusters have been previously demonstrated,[18,19] ESI-MS and ESI-MS/MS have revealed in the present case as essential to determine the nature of the species in solution. ESI-MS and its tandem version are rapidly becoming the technique of choice for mechanistic and speciation studies of metal complexes and have appeared in the last years as a breakthrough for the rapid and sensitive characterization of organometallic compounds.[20–24] In this sense, the results in the present work provide an excellent example of the utility of this multilateral approximation in speciation and mechanistic studies.

2 Results and discussion

2.1 Synthesis and crystal structure of $[W_2Se_2(\mu\text{-}Se)_2(\mu\text{-}CH_3CO_2)(dmpe)_2]PF_6$ ($[\mathbf{2}]PF_6$)

Reaction of the trinuclear W(IV) complex $[W_3Se_4(OH)_3(dmpe)_3]PF_6$ ($[\mathbf{1}]PF_6$) with acetic acid in boiling acetonitrile results in a colour change from green to red to give $[W_2Se_2(\mu\text{-}Se)_2(\mu\text{-}CH_3CO_2)(dmpe)_2]PF_6$ ($[\mathbf{2}]PF_6$) in 42% yield. Identification of other species (presumably one or several mononuclear complexes) has not been elucidated yet on the basis of ^{31}P NMR and ESI-MS, which indicates that other products formed in the reaction are either paramagnetic or insoluble in the reaction media. Formation of $[\mathbf{2}]^+$ indicates that the reaction occurs through cluster fragmentation, the trinuclear starting complex being converted to a dinuclear species. Fragmentation reactions of transition metal clusters represent a widely used synthetic entry for the preparation of lower nuclearity complexes. These kinds of reactions are considered "rational" because the products formed contain previously preassembled structural motifs in the starting material. In some cases this route has proved to be superior to building-block or excision synthetic methodologies.[25,26] In a previous work we outlined the usefulness of degradation reactions starting from cluster complexes of molybdenum and tungsten with M_3Q_4 (M = Mo, W; Q = S, Se) cores bearing 1,2-bisdithiolene ligands to give the family of complexes of general formula $[M_2O_2(\mu\text{-}Q)_2(1,2\text{-dithiolene})_2]^{2-}$.[27] In the present case, this route is especially valuable since dinuclear selenium complexes with $[W_2Se_2(\mu\text{-}Se)_2]$ cluster cores are scarce. A family of compounds of general formula $[W_2Se_2(\mu\text{-}Se)_2(Se_n)_2]^{2-}$ (n = 2, 3, 4) was prepared by Ibers and co-workers in 1988 where often the presence of several isomers coexist with higher nuclearity compounds.[28–30]

The structure of complex $[\mathbf{2}]PF_6$ has been determined by single crystal X-ray diffraction. Compound $[\mathbf{2}]PF_6$ crystallizes in the chiral space group $P2_1$. Fig. 1 shows the ORTEP representation with the atom numbering scheme.

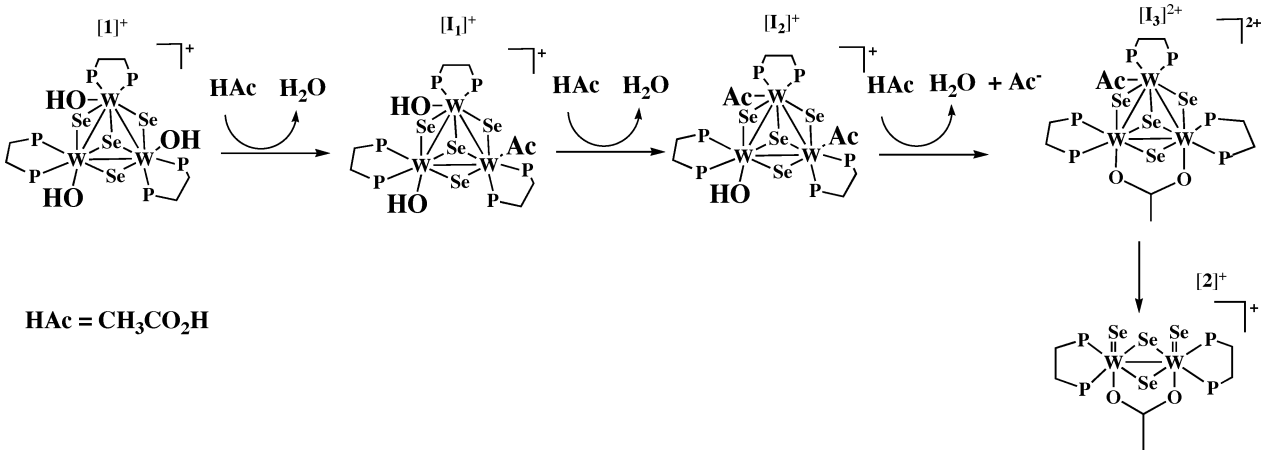

Scheme 1

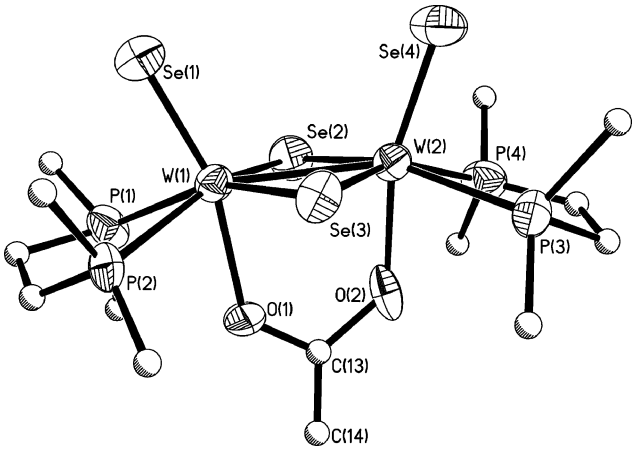

Fig. 1 ORTEP representation (50% thermal probability ellipsoids) of cation $[\mathbf{2}]^+$ with the atom numbering scheme. Carbon atoms are drawn as spheres for clarity.

The compound has both metal centers connected through two bridged selenido groups, each metal appearing as six-coordinated in a distorted octahedral environment without considering the metal–metal interaction. The remaining positions on each metal are occupied by the two diphosphane phosphorus atoms, one oxygen atom from the bridging acetate ligand and one terminal selenium atom. The terminal selenium atoms in $[\mathbf{2}]^+$ are in a *syn* configuration with the two diphosphane molecules bent with respect to the plane defined by the central $W_2(\mu\text{-}Se)_2$ unit and pointing away the terminal selenium atoms. This arrangement is also found in the dinuclear complex $(Et_4N)[Mo_2O_2(\mu\text{-}S)_2(\mu\text{-}CF_3CO_2)(S_2P(OEt)_2)_2]$ and other closely related complexes of general formula $[Mo_2X_2(\mu\text{-}Q)_2L_2]$ (X = O, S, Se; Q = S, Se; L = bidentate ligand).[29–36] Table 1 shows a list of selected bond lengths in compound $[\mathbf{2}]PF_6$ together with those of other dinuclear complexes containing similar $W_2Q_2(\mu\text{-}Se)_2$ (Q = O, Se) cluster cores.

The W–W bond distance in $[\mathbf{2}]PF_6$ is consistent with an oxidation state of +5 for the metal and the presence of a single metal–metal bond. The metal–metal bond in $[\mathbf{2}]PF_6$ is slightly shorter than equivalent distances in other analogous compounds, but similar W=Se bond distances are observed for the whole series. The W–(μ-Se) distances are increased by *ca.* 0.04 Å in the diphosphane-containing complexes, which is also reflected in a closure of the W–(μ-Se)–W angle. The most significant difference with other complexes listed in Table 1 is observed in the dihedral angle (Π) within the central $W_2(\mu\text{-}Se)_2$ unit, which is almost planar in $[\mathbf{2}]PF_6$. Theoretical calculations carried out on a series of dithiolene complexes with $M_2(\mu\text{-}S)_2$ (M = Mo, W) cores predict a completely planar arrangement only for those complexes possessing a *trans* configuration with respect to the terminal atoms.[32] In fact, a detailed crystallographic analysis of all other complexes with $M_2(\mu\text{-}Q)_2$ (M = Mo, W; Q = O, S, Se) cores and bidentate ligands, including either five- and six-coordinated metal atoms, show dihedral angles typically in the 135–155° range.[37] Therefore, the $[\mathbf{2}]^+$ cation can be considered as a rare example where the planarity of the $W_2(\mu\text{-}Se)_2$ unit coexists with the syn configuration of the terminal ligands. We speculate that the accommodation of the bridging selenium atoms on the side where the diphosphanes molecules are bent is sterically unfavored, thus the bridging selenium atoms are forced to be in the metal plane.

2.2 The reaction of $[W_3Se_4(OH)_3(dmpe)_3]^+$ with CH_3CO_2H in CH_3CN solution: kinetics of reaction and the nature of intermediates

The reaction of complex $[\mathbf{1}]^+$ with acetic acid to yield $[\mathbf{2}]^+$ is completed in 1 h in boiling acetonitrile. However, with the aim to identify reaction intermediates leading to such transformation, the reaction was also monitored at room temperature where it proceeds smoothly and is completed in five days. Stopped-flow experiments at 25.0 °C showed that reaction of cluster $[\mathbf{1}]^+$ with an excess of acetic acid in acetonitrile solution yields complex spectral changes that require a model with three consecutive steps for a satisfactory fit (eqn (1)). The analysis of the experimental data with this model provides the values of the observed rate constants for the three steps (k_{1obs}, k_{2obs} and k_{3obs}) as well as calculated spectra for the several species involved (see Fig. 2). It is important to note that the spectrum calculated for the species formed in the third step does not correspond with that of $[\mathbf{2}]PF_6$, and that slower spectral changes following the third step reveal the existence of an additional chemical process out of the stopped-flow time scale. In consequence, the last stages of the reaction have been monitored with a conventional UV-vis spectrophotometer where cation $[\mathbf{2}]^+$ has been identified as the final reaction product, although the values of the rate constants are still not well-behaved.

$$[\mathbf{1}]^+ + CH_3CO_2H_{exc} \rightarrow \mathbf{I_1} \rightarrow \mathbf{I_2} \rightarrow \mathbf{I_3} \rightarrow \text{slower changes} \quad (1)$$

The rate constants for the first three resolved steps are independent of the cluster concentration but show a linear dependence with respect to the acetic acid concentration (Fig. 3). The fit of the data by eqn (2) leads to the following values of the corresponding second-order rate constants: $k_1 = 20 \pm 1\ M^{-1}\ s^{-1}$; $k_2 = 0.37 \pm 0.02\ M^{-1}\ s^{-1}$ and $k_3 = 0.139 \pm 0.002\ M^{-1}\ s^{-1}$.

$$k_{iobs} = k_i[CH_3COH];\ i = 1, 2, 3 \quad (2)$$

Table 1 Selected averaged bond distances (Å), W–$Se_{bridged}$–W angle (°) and dihedral angle Π between the two W(μ-Se_2) planes (°) for compounds $[\mathbf{2}]PF_6$, $(PPh_4)_2[W_2O_2(\mu\text{-}Se)_2(dmit)_2]$, $(PPh_4)_2[W_2Se_2(\mu\text{-}Se)_2(Se_3)_2]/(PPh_4)_2[W_2Se_2(\mu\text{-}Se)_2(Se_2)(Se_4)]$ and $(PPh_4)_2[W_2Se_2(\mu\text{-}Se)_2(Se_2)(Se_4)]/(PPh_4)_2[W_2Se_2(\mu\text{-}Se)_2(Se_2)(Se_3)]$[a]

	W–W	W=Se	W–$Se_{bridged}$	W–$Se_{bridged}$–W	Π[b]	Ref.
$[W_2Se_2(\mu\text{-}Se)_2(\mu\text{-}CH_3CO_2)(dmpe)_2]PF_6$	2.848(2)	2.270[4]	2.476[9]	70.2[4]	177.0	This work
$(PPh_4)_2[W_2O_2(\mu\text{-}Se)_2(dmit)_2]$	2.8715(14)		2.441[9]	72.1[2]	135.5	27
$(PPh_4)_2[W_2Se_2(\mu\text{-}Se)_2(Se_3)_2]/(PPh_4)_2[W_2Se_2(\mu\text{-}Se)_2(Se_2)(Se_4)]$[b]	2.903(2)	2.250[3]	2.45[4]	72.6[8]	153.7	29
$(PPh_4)_2[W_2Se_2(\mu\text{-}Se)_2(Se_2)(Se_4)]/(PPh_4)_2[W_2Se_2(\mu\text{-}Se)_2(Se_2)(Se_3)]$[b]	2.897(2)	2.25[1]	2.45[4]	72.49[2]	153.8	29

[a] Averaged values are indicated with square brackets. [b] Both compounds appear co-crystallized.

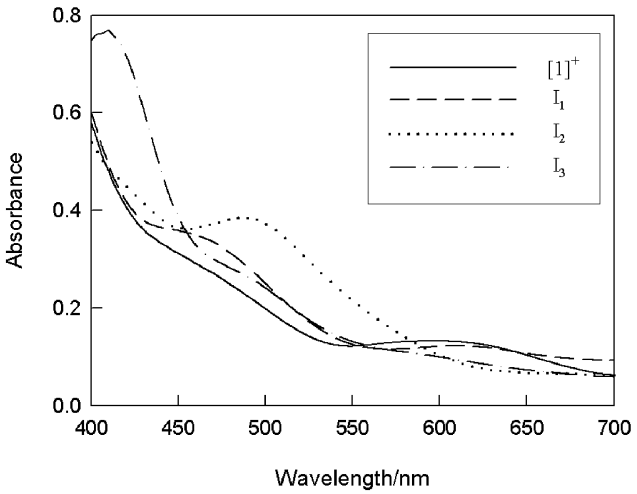

Fig. 2 Spectra calculated from the spectral changes observed in the stopped-flow experiments for the intermediates formed in the reaction of $[\mathbf{1}]^+$ with acetic acid in acetonitrile solution.

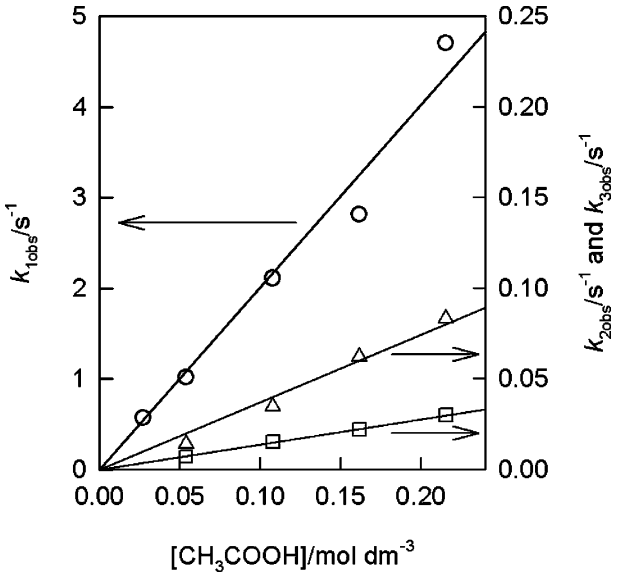

Fig. 3 Plots showing the dependence with the acid concentration for the rate constants corresponding to the first three steps in the reaction of $[\mathbf{1}]^+$ with acetic acid in acetonitrile solution. Note that the scale used for k_{1obs} (circles) is different from that used for k_{2obs} (triangles) and k_{3obs} (squares).

To obtain information about the nature of the intermediates, the reaction of cluster $[\mathbf{1}]^+$ with acetic acid was monitored using $^{31}P\{^1H\}$ NMR spectroscopy as described in the Experimental section. The $^{31}P\{^1H\}$ NMR spectra of cluster $[\mathbf{1}]^+$ shows a two signals pattern consistent with its incomplete-cuboidal type structure, where the two signals correspond to the two sets of phosphorus atoms located above and below (*trans* to the (μ-Se) and (μ_3-Se) ligand) the metal plane. During the early stages of the reaction, the signals of the starting complex (14.0 and −6.0 ppm) coexist with six new signals at 13.2, 10.8, 8.9, 1.5, −2.4 and −8.2 ppm. When the reaction progresses, the latter signals increase in intensity while those of the starting complex decrease, thus showing that the new signals correspond to intermediate $\mathbf{I_1}$. The observation of six signals for intermediates formed in the reactions of these clusters has been previously reported and interpreted as the result of the symmetry decrease due to ligand substitution at a single metal site, which breaks the overall C_3 symmetry making non equivalent the six phosphorous atoms of the diphosphane ligands.[19,38] At later stages of the reaction, there is a decrease in the intensity of the signals for $\mathbf{I_1}$ with appearance of six new signals at 21.9, 18.3, 17.4, 13.7, 4.8 and −3.0 ppm. The latter signals can be assigned to intermediate $\mathbf{I_2}$ and must correspond to the product resulting from the reaction at two metal centres, which still maintains the symmetry decrease.

In a further step, four new signals are observed at 29.7, 13.4, 11.2 and 8.9 ppm and assigned to intermediate $\mathbf{I_3}$, where the intensities of the two central signals approximately double those of the other two. We have not previously observed any four-signal spectrum for reaction intermediates coming from this kind of trimetallic clusters. This characteristic $^{31}P\{^1H\}$ spectrum suggests an overall C_2 symmetry for the $\mathbf{I_3}$ intermediate, consistent with the presence of two equivalent metal sites in the cluster core. However, the possibility that this pattern results from the accidental simplification of a standard six-signal spectrum cannot be definitely ruled out. For example, the $^{31}P\{^1H\}$ spectra of the family of carboxylate-bridged trinuclear complexes of general formula $[Mo_3S_4(\mu\text{-}RCO_2)(dtp)_3L]$ ($dtp = S_2P(OEt)_2$; $R = CH_3$, *p*-ClC_6H_4 or *p*-$NO_2C_6H_4$, L = solvent) reveal the presence of only two inequivalent dtp ligands despite the overall C_s symmetry.[39–41] In any case, the identification of $\mathbf{I_3}$ as the product of the reaction at the third metal site can be definitively ruled out as the recovery of the C_3 symmetry would result in the characteristic two signal pattern observed for compound $[\mathbf{1}]^+$. Addition of a large excess of acid generates intermediate $\mathbf{I_3}$ together with small amounts of the $[\mathbf{2}]^+$ cation within 2–3 h. This cation presents a single signal in the $^{31}P\{^1H\}$ spectrum at 29.4 ppm which coexist in some cases with another one at 23.8 ppm associated to the closely-related oxo-terminal product of formula $[W_2O_2(\mu\text{-}Se)_2(\mu\text{-}CH_3CO_2)(dmpe)_2]^+$ (see below). The relative intensities of the signals at 29.4 and 23.8 ppm change with time and also between different preparations, in agreement with the lack of reproducibility of the kinetic data for the last stages of the reaction.

The NMR data described above provides key information on the nature of these intermediates since they allow the identification of the cluster core overall symmetry. However these experiments do not provide information on the nature of the ancillary ligands in each intermediate, and the proton spectra are too complex to be resolved. To overcome such limitation, we decided to carry out detailed ESI-MS and ESI-MS/MS experiments to get a complete picture of the intermediates involved in the different steps. The positive-mode ESI-MS spectra of the starting compound $[\mathbf{1}]^+$ in acetonitrile is shown in Fig. 4 (bottom).

The ESI-MS reveals two major peaks which corresponds to the single-charged molecular peak $[\mathbf{1}]^+$ (m/z = 1367.8 u) and the doubly-charged $[\mathbf{1} - OH]^{2+}$ ion (m/z = 676.0 u). Additionally, less intense peaks corresponding to the solvated $[\mathbf{1} + H_2O]^+$ (m/z = 1395.8 u) and the protonated $[\mathbf{1} + H]^{2+}$ (m/z = 685.0 u) molecular ion are also observed. The presence of the doubly-charged $[\mathbf{1} - OH]^{2+}$ and $[\mathbf{1} + H]^{2+}$ species may be attributed to the gas-phase protonation, most likely at one terminal OH^- ligand to give the $[\mathbf{1} + H]^{2+}$ ion that partially dissociates water to yield the $[\mathbf{1} - OH]^{2+}$ species. However, as the phosphorus spectrum of acetonitrile solutions of $[\mathbf{1}]^+$ show exclusively the two signals expected for the three equivalent diphosphane ligands, it must be

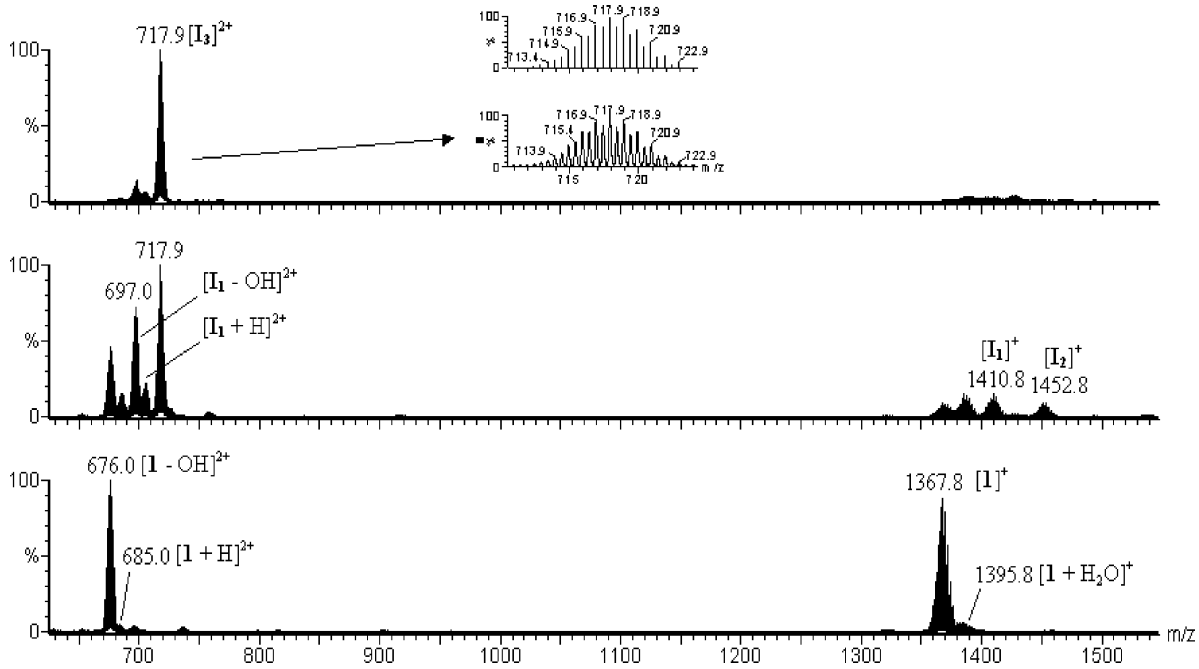

Fig. 4 ESI-MS spectra for compound [**1**]PF_6 in acetonitrile (bottom) and after addition of three equivalents (middle) and a ten-fold excess of acetic acid (top). The inset shows the simulated and experimental isotopic pattern for the intermediate $[\mathbf{I_3}]^{2+}$.

concluded that these acid–base reactions only occur in the gas phase. Although these processes can complicate the interpretation of the spectra and identification of intermediates in solution, it was found that ESI-MS is of great utility in this field. For this purpose, controlled amounts of acetic acid were added in a way similar to that used for some of the NMR experiments, which allowed stopping the reaction at different stages. It is important to note that the nature of the intermediates detected showed no variation neither with concentration (dilution with acetonitrile to a final concentration ranging from 1×10^{-3} to 1×10^{-5} M yielded identical ESI mass spectra) nor time, indicating that formation of new species occurs rapidly in the time scale of sample manipulation for this experimental technique. Scheme 1 shows a diagram of the intermediates captured and identified on the basis of ESI-MS and $^{31}P\{^1H\}$ NMR analysis.

The ESI mass spectrum obtained after addition of three equivalents of acetic acid is shown in Fig. 4 (middle). It is clearly seen that the presence of doubly-charged species is predominant. This is a consequence of the acidic media conditions which favor the protonation of the hydroxyl groups and promote ionisation processes that lead to major signals for species of general formula $[\mathbf{M} - OH]^{2+}$. The intensity of the signals ($[\mathbf{1}]^+$ and $[\mathbf{1} - OH]^+$) for the unmodified starting species is dramatically reduced relative to the new appearing species that correspond to the replacement of one and two hydroxyl ligands by acetate groups (intermediates labelled as $[\mathbf{I_1}]^+$ and $[\mathbf{I_2}]^+$ in Fig. 4). These intermediates are identified as single-charged species, namely $[W_3Se_4(OH)_2(CH_3CO_2)(dmpe)_3]^+$ $[\mathbf{I_1}]^+$ (peak centered at m/z = 1410.8 u) and $[W_3Se_4(OH)(CH_3CO_2)_2(dmpe)_3]^+$ $[\mathbf{I_2}]^+$ (peak centered at m/z = 1452.8 u). A set of intense doubly-charged peaks are also detected as a result of the gas-phase protonation and water-releasing of intermediates $[\mathbf{I_1}]^+$ and $[\mathbf{I_2}]^+$, namely $[W_3Se_4(OH)(CH_3CO_2)(dmpe)_3]^{2+}$ $[\mathbf{I_1} - OH]^{2+}$ (peak centred at m/z = 697.0 u), and $[W_3Se_4(CH_3CO_2)_2(dmpe)_3]^{2+}$ $[\mathbf{I_2} - OH]^{2+}$ (peak centred at m/z = 717.9 u). Minor signals due to the presence of gas-phase protonated $[\mathbf{1} + H]^{2+}$ (peak centered at m/z = 685.0 u) and $[\mathbf{I_1} + H]^{2+}$ (peak centred at m/z = 703.9 u) are also observed.

Fig. 4 (top) shows the ESI mass spectra after addition of a ten-fold excess of acetic acid. The formation of a single peak centred at 717.9 u $[W_3Se_4(CH_3CO_2)_2(dmpe)_3]^{2+}$ is observed together with the disappearance of the starting precursor $[\mathbf{1}]^+$ and the remaining intermediates. It is interesting to note the absence of protonated species of formula $[\mathbf{M} + H]^{2+}$ (expected m/z = 725.9 u) for this intermediate. This experimental evidence indicates that this intermediate does not contain hydroxyl groups in the cluster core since it is a pre-requisite for protonation. On the basis of this assumption, the doubly-charged species at m/z = 717.9 previously assigned to $[\mathbf{I_2} - OH]^+$ must be reformulated as corresponding to an unsaturated complex $[\mathbf{I_3}]^{2+}$ of formula $[W_3Se_4(CH_3CO_2)_2(dmpe)_3]^{2+}$ or its acetate-bridged $[W_3Se_4(CH_3CO_2)(\mu\text{-}CH_3CO_2)(dmpe)_3]^{2+}$ isomer. As we mentioned above, the observation of four phosphorus signals for this intermediate suggests the existence of two equivalent metal centres, which favors the latter formulation provided that the bridging acetate forces the reorganisation of the coordination environment about the two bridged metal centres making them equivalent. In agreement with the NMR results, no signals for the $[W_3Se_4(CH_3CO_2)_3(dmpe)_3]^+$ species are observed in the ESI-MS experiments, although formation of this tri-substituted complex should be reasonably expected from the previously reported chemistry of this kind of cluster with ligands such as Cl^- and Br^-.[18,19] After allowing to stand the reaction mixture for five days the presence of peaks corresponding to compound $[\mathbf{2}]^+$ (signal centered at m/z = 1043.0 u) together with minor formation of $[W_2O_2(\mu\text{-}Se)_2(\mu\text{-}CH_3CO_2)(dmpe)_2]^+$ (signal centered at m/z = 917.0 u) are observed. These results agree with the $^{31}P\{^1H\}$ NMR

data described above, in which two phosphorous signals are observed in the later stages of the reaction.

The elemental composition of all intermediates captured can be established from the analysis of their isotopic pattern. A representative ESI mass spectra for the intermediate $[\mathbf{I_3}]^{2+}$ is shown in Fig. 4, where the excellent agreement between the experimental and calculated isotopic distribution is observed. ESI-MS/MS analysis was also used as a structural diagnostic tool which provided further information on the molecular organization of the captured intermediates. In all cases a well-defined fragmentation pathway is observed for the gas-phase species generated from $[\mathbf{1}]^+$, $[\mathbf{I_1}]^+$, $[\mathbf{I_2}]^+$, $[\mathbf{I_3}]^{2+}$ and $[\mathbf{2}]^+$ according to previously reported gas-phase fragmentation studies on related complexes.[42] These results support the assignment postulated in the preceding paragraphs (see supporting information).

Species generated from $[\mathbf{1}]^+$, namely $[\mathbf{1}]^+$ and $[\mathbf{1} - \mathrm{OH}]^{2+}$ liberate one diphosphane ligand together with one water molecule under ESI-MS/MS conditions. Species generated from $[\mathbf{I_1}]^+$, namely $[\mathbf{I_1}]^+$ and $[\mathbf{I_1} - \mathrm{OH}]^{2+}$ dissociate one diphosphane ligand together with one water and one acetic acid molecule. Species $[\mathbf{I_2}]^+$ ejects one diphosphane ligand together with two acetic acid molecules, whereas $[\mathbf{2}]^+$ dissociates one diphosphane ligand together with one ketene CH_2CO molecule. A correlation between the coordination mode of the acetate ligand and the identity of the neutral fragments evolved is clearly seen: the terminal acetate ligands are converted to CH_3CO_2H whereas the bridging acetate gives CH_2CO. From these results, relevant information is extracted from ESI-MS/MS experiments of species $[\mathbf{I_3}]^{2+}$ (see Fig. 5)

Beside the loss of one diphosphane molecule, two different fragmentation channels are observed for the two acetate ligands. One of them yields CH_2CO whereas the remaining one dissociates CH_3CO_2H, in agreement with the proposed formulation depicted in Scheme 1. Although this gas-phase behaviour for the "W–acetate" functional groups is valid in the present case, it cannot be extended to other related complexes. For example the acetate terminal species $[W_2O_6(CH_3CO_2)]^+$ dissociates through ketene expulsion in sharp contrast with the fragmentation pathway described above.[14] These results put forward that the identity of the peripheral ligands can play a determining role on the preferred fragmentation pathway.

2.3 Reaction mechanism

According to the results of the NMR, ESI-MS and ESI-MS/MS experiments, the three resolved kinetic steps can be represented as follows:

$$[W_3Se(OH)_3(dmpe)_3]^+ ([\mathbf{1}]^+) \rightarrow [W_3Se_4(OH)_2(Ac)(dmpe)_3]^+ ([\mathbf{I_1}]^+) \quad (3.1)$$

$$[W_3Se_4(OH)_2(Ac)(dmpe)_3]^+ ([\mathbf{I_1}]^+) \rightarrow [W_3Se_4(OH)(Ac)_2(dmpe)_3]^+ ([\mathbf{I_2}]^+) \quad (3.2)$$

$$[W_3Se_4(OH)(Ac)_2(dmpe)_3]^+ ([\mathbf{I_2}]^+) \rightarrow [W_3Se_4(OH)(Ac)(\mu\text{-}Ac)(dmpe)_3]^{2+} ([\mathbf{I_3}]^{2+}) \quad (3.3)$$

The formation of the dinuclear product $[\mathbf{2}]^+$ occurs in a slower step. With regards to the nature of the processes occurring in each one of the steps, one important point is the nature of the attacking species because all three steps show a first-order dependence with respect to the total concentration of the acid. Acetic acid behaves as a very weak acid in acetonitrile solution ($pK_a = 22.3$),[43] so that it remains essentially undissociated. Although homoconjugation is also possible in this solvent [$\log K_f (HAc_2^-) = 3,8$],[43] the low degree of dissociation makes the amount of HAc_2^- negligible in the absence of added acetate anion. Because of the extremely low concentrations of Ac^- and HAc_2^-, it appears reasonable to think of molecular HAc as the attacking species in the three resolved kinetic steps. The first two steps would then involve the sequential substitution of two coordinated OH^- groups by acetate ligands coming from acetic acid. These substitutions surely go through acid attack to OH^- with water

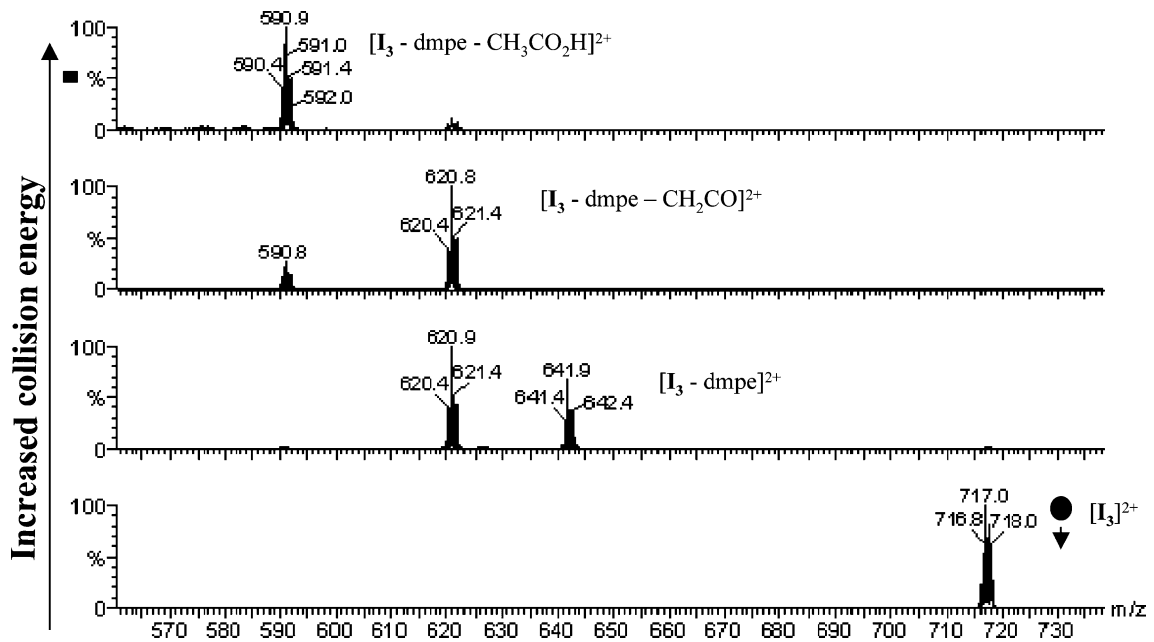

Fig. 5 Product ion mass spectrum for the mass-selected $[W_3Se_4(OH)(Ac)(\mu\text{-}Ac)(dmpe)_3]^{2+}$ ($[\mathbf{I_3}]^{2+}$) cluster centred at m/z 717.9.

elimination and further coordination of the acetate anion. The acid-promoted substitution of coordinated ligands in solution is well documented[44] and it has been also observed in the gas phase for the reaction of $[Mo_2O_6(OH)]^{2-}$ and related complexes with acetic acid and alcohols.[12–14] However, the third step does not involve the coordination of an acetate group but the bridging mode coordination of one of the previously coordinated acetate ligand. The first order dependence of this step (k_{3obs}) with respect to CH_3CO_2H appears because a molecule of acid is needed to protonate the remaining OH^- ligand, although coordination of the acetate anion formed in this process does not occur. This apparent contradiction can be rationalised taking into consideration that two competitive processes for the $CH_3CO_2^-$ attack (K_{2obs} and K_{3obs}) may follow the coordination of the first acetate ligand. In both processes the hydroxo group is protonated but in one case, the resulting acetate ligand coordinates to the metal while in the other case, coordination comes from a previously bounded acetate that act as a bridging ligand between two tungsten atoms. The predominant species depends on the relative rates of both processes and on the basis of the previously discussed results we can state that bridge formation is slower than acetate coordination. However, the ratio between the rate constants for the first two steps has a value ($k_1/k_2 = 54$) that clearly indicates an important deviation from the statistical prediction ($k_1/k_2 = 3/2 = 1.5$). Although the comprehensive work carried out by the group of Sykes firmly established the operation of statistical kinetics for the substitution reactions of this kind of cluster, it is important to note that this conclusion is derived from the study of water substitution in aqueous solution using $[M_3Q_4(H_2O)_9]^{4+}$ and related aqua-clusters.[45–47] However, in a recent study we have found that the kinetics of reaction of $[W_3S_4H_3(dmpe)_3]^+$ with HCl in CH_2Cl_2 significantly deviates from the statistical behaviour.[38] The results in the present work seem to indicate that this kind of deviation can be quite common in the reaction of these clusters when water is changed by other solvents and ligands.

The significant decrease from the statistical prediction observed for the second step anticipates a drastic deceleration of the process leading to formation of $[\mathbf{I_3}]^{2+}$ in the third step. From the values of k_1 and k_2, it can be estimated that the value of k_3 for coordination of the third acetate should be lower than 10^{-3} M^{-1} s^{-1}, thus making this pathway slower than bridge formation, which occurs with $k_3 = 0.139$ M^{-1} s^{-1}.

With regards to the final conversion of $[\mathbf{I_3}]^{2+}$ to $[\mathbf{2}]^+$, the difficulties found for studying the kinetics of reaction and the absence of information about the mononuclear complex formed with the metal centre released from the cluster preclude a satisfactory explanation. As no intermediate is observed between $\mathbf{I_3}$ and $[\mathbf{2}]^+$ in the NMR and ESI-MS experiments, it can be speculated that a new CH_3CO_2H attack to the W of $\mathbf{I_3}$ not involved in the acetate bridge starts a cascade of processes that finally result in dissociation of this metal centre. As completion of the reaction requires the breaking of several W–ligand bonds, the activation energy must be high and the process is significantly slower than the first three steps in the reaction of $[\mathbf{1}]^+$ with acetic acid. Given the interest in understanding the fragmentation processes in these clusters and the potential usefulness of the dinuclear complex as a synthon for synthetic building-block strategies, more work is currently being carried out on these systems and the results will be reported in the future.

3 Conclusions

The acetic-acid mediated degradation of the trinuclear $[W_3Se_4(OH)_3(dmpe)_3]^+$ compound is a convenient synthetic entry to the dinuclear $[W_2Se_2(\mu\text{-}Se)_2(\mu\text{-}CH_3CO_2)(dmpe)_2]^+$ $[\mathbf{2}]^+$ complex. The mechanistic picture and identity of the intermediates involved in such degradation have been investigated through a combined study using stopped-flow, ^{31}P NMR, ESI-MS and ESI-MS/MS spectrometric techniques.

Three steps can be distinguished in the stopped-flow time scale, all of them showing a first order dependence with respect to the acid. These studies indicate that the first two steps correspond to the sequential coordination of acetate ligands at two metal centres evolving water. The third step involves bridging of one of the terminal acetate ligands, which actually prepares the trinuclear cluster to afford the acetate-bridged $[W_2Se_2(\mu\text{-}Se)_2(\mu\text{-}CH_3CO_2)(dmpe)_2]^+$ ($[\mathbf{2}]^+$) complex. Closely related synthetic entries to dinuclear $W_2O_2(\mu\text{-}Se)_2$ and trinuclear W_3Se_4 complexes based on cluster fragmentation have been reported.[26,27] In these cases, the presence of oxygen was required to dismantle the W_3Se_4 and W_4Se_4 starting materials. In the present case, fragmentation proceeds under inert conditions, thus the presence of internal redox processes within the trinuclear W_3Se_4 core can be invoked as the driving force for metal cluster fragmentation. Despite the only product detected is the $[\mathbf{2}]^+$dimer, the following redox conversion $[W(IV)]_3 \rightarrow [W(V)]_2 + W(III)$ is tentatively proposed

4 Experimental

4.1 Synthesis of $[W_2Se_2(\mu\text{-}Se)_2(\mu\text{-}CH_3CO_2)(dmpe)_2]PF_6$ $[\mathbf{2}]PF_6$

To a green solution of $[\mathbf{1}]PF_6$ (0.070 g, 0.046 mmol.) in acetonitrile (10 mL) was added a ten-fold excess of acetic acid and the mixture was heated at 50 °C for 1 h under an inert atmosphere. A progressive colour change is observed from green to red. Addition of 200 mL of diethyl ether causes the precipitation of a red solid which was filtered. This precipitate was redissolved in dichloromethane and loaded onto a silica gel column. After washing with CH_2Cl_2, elution with acetone yielded a concentrated red solution which was taken to dryness, filtered and slow diffusion of diethyl ether gave compound $[\mathbf{2}]PF_6$ as a microcrystalline red powder (24 mg, 42%) (Found: C, 14.03; H, 2.96, O 2.97. $W_2Se_4C_{14}H_{35}P_3F_6O_2$ requires C, 14.16; H 2.97, O 2.69%). IR (KBr) cm^{-1}: 1720 (s, C=O), 1420 (s); 1286 (s), 1073 (m), 937 (m), 840 (s, P–F), 652 (w), 556 (m, P–F), 315 (s); ^1H NMR: δ (CD_3CN) (ppm): 1.48 (d, $^2J_{PH} = 11$ Hz, $CH_{3\,diphosphane}$), 2.33 (s, $CH_{3\,acetate}$), 2.47 (m, $CH_{2\,diphosphane}$), 2.81 (m, $CH_{2\,diphosphane}$), 2.95 (d, $^2J_{PH} = 10$ Hz, $CH_{3\,diphosphane}$); $^{13}C\{^1H\}$ NMR: δ (CD_3CN) (ppm): 15.5 (d, $^1J_{PC} = 6$ Hz, $CH_{3\,diphosphane}$), 21.5 (s, $CH_{3\,acetate}$) 27.1 (d, $^1J_{PC} = 7$ Hz, $CH_{3\,diphosphane}$), 29.9 (d, $^1J_{PC} = 4$ Hz, $CH_{2\,diphosphane}$); $^{31}P\{^1H\}$ NMR: δ (CD_3CN) (ppm): 29.4 (s, $^1J_{PW} = 174.3$ Hz), −143.93 (septet, $^1J_{P-F} = 705.8$). ESI-MS(+) m/z: 1042.8 $[M]^+$.

4.2 Kinetic experiments

Solutions for the kinetic studies were prepared by dissolving $[\mathbf{1}]PF_6$ in acetonitrile, the complex concentration being 2.0×10^{-3} mol dm^{-3}. These solutions were mixed in the stopped-flow instrument with solutions containing acetic acid in the same solvent. All the experiments were carried out at 25.0 °C under

pseudo-first order conditions of acid excess in the presence of 0.1 M Et_4NBF_4. The reaction kinetics was monitored by recording the spectral changes with time using an Applied Photophysics SX17MV stopped-flow instrument provided with a PDA.1 diode array detector. The experimental data were analyzed with program SPECFIT,[48] and a satisfactory fit was obtained by using a model with three consecutive exponentials. The first order dependence of the three observed rate constants with respect to the complex concentration was confirmed by the lack of changes of their numerical values when the complex concentration (deficit) was changed. The first order dependence with respect to acetic acid was determined by analyzing the changes of the rate constants when the concentration of acetic acid (excess) was changed. Attempts to follow the kinetics of the slower spectral changes leading to formation of $[\mathbf{2}]^+$ were carried out with a Cary 50 BIO Uv-Vis spectrophotometer using experimental conditions and fitting procedures similar to those used for the stopped-flow experiments.

4.3 NMR monitoring of the reaction

For this purpose, some experiments were carried out by adding an excess of the acid to a sample of the complex previously cooled at −35 °C in the NMR spectrometer and then recording several successive spectra at this low temperature. When no spectral changes are observed within a reasonable time (*ca.* 30 min.), the sample was warmed up to −15 °C and new spectra recorded, the procedure being repeated until achieving 25 °C. These low temperature experiments using an excess of acetic acid were complemented with other experiments in which deficits of acetic acid were added to the complex at 25 °C, in such a way that controlling the amount of acid added allows stopping the reaction at different stages. The results obtained from both types of experiment were consistent with each other, thus providing a complete picture of the NMR spectra of the different intermediates involved in the reaction. $^{31}P\{^1H\}$ NMR were recorded on a Varian INOVA 400 MHz instrument using CD_3CN as solvent and were referenced to external 85% H_3PO_4. ^1H, $^{13}C\{^1H\}$ and ^1H–^{13}C gHSQC spectra were recorded on a Varian INOVA 500 MHz instrument. Chemical shifts are reported in parts per million from tetramethylsilane with the solvent resonance as the internal standard.

4.4 Electrospray-mass spectrometry

A hybrid QTOF I (quadrupole–hexapole–TOF) mass spectrometer with an orthogonal Z-spray-electrospray interface (Micromass, Manchester, UK) was used. Mass calibration was performed daily using a solution of sodium iodide in isopropanol–water (50 : 50) from *m/z* 100 to 1900 u. Sample solutions were infused *via* syringe pump directly connected to the ESI source at a flow rate of 10 μL min^{-1}. The observed isotopic pattern of each intermediate perfectly matched the theoretical isotope pattern calculated from their elemental composition using the MassLynx 4.0 program. Some considerations are necessary to asses the identification of species present in solution on the basis on ESI-MS. This soft technique is amongst the less intrusive mass spectrometric techniques, although it is well documented that the ionization process may still induce fragmentation or rearrangement processes as well as solvation of the target compound, thus resulting in the observation of species not present in solution. In these cases, careful optimization of the experimental conditions is required in order to find the analytical conditions leading to spectra that most closely resemble the speciation chemistry in solution. Preliminary ESI-MS experiments were conducted by reacting increasing amounts of acetic acid with sample solutions of $[\mathbf{1}]^+$ in acetonitrile. In these experiments, the operating conditions of the mass spectrometer had to be finely tuned. In the present study the use of low desolvation gas and source temperature, (i.e 100 and 70 °C, respectively) resulted in the presence of very crowded spectra due to the presence of acetonitrile or water solvated species. The use of higher temperatures in the ESI chamber typically favors condensation and desolvation reactions of the ionized species. In the present study, optimal conditions were found at temperatures of 250 and 120 °C for the desolvation gas and source temperature, respectively. At these conditions, the presence of solvated species was decreased considerably, thus resulting in less crowded ESI spectra. The capillary voltage had a negligible effect on the abundance of the intermediates detected, but the cone voltage was necessarily kept to a low value (5 V) to control the extent of fragmentation of the species observed. Tandem MS/MS spectra were obtained at various collision energies (typically in the range 0–50 eV) by selecting the precursor ion of interest with the first quadrupole (Q1) with an isolation width of approximately 2 Da and scanning with the time of flight analyzer (TOF). Argon was used as collision gas and the pressure in the collision cell was maintained at 4×10^{-5} mbar.

4.5 Other physical measurements

Elemental analysis were performed on an EA 1108 CHNS microanalyzer. IR spectra were recorded on a Perkin-Elmer System 2000 FT-IR instrument using KBr pellets.

4.6 X-Ray crystallography

Suitable crystals for X-ray studies for compound $[\mathbf{2}]PF_6$ were grown by slow diffusion of diethyl ether into sample solutions in CH_2Cl_2. The data collection was performed on a Bruker Smart CCD diffractometer using graphite-monochromated Mo-Kα radiation ($\lambda = 0.71073$ Å) with a nominal crystal-to-detector distance of 4 cm. A hemisphere of data was colleted based on three ω-scan runs (starting $\omega = -28°$) at values $\phi = 0$, 90 and 180° with the detector at $2\theta = 28°$. At each of these runs, frames (606, 435 and 230 respectively) were collected at 0.3° intervals and 35 s per frame. The diffraction frames were integrated using the SAINT package and corrected for absorption with SADABS.[49,50] The positions of the heavy atoms were determined by direct methods and successive difference electron density maps using the SHELXTL 5.10 software package were done to locate the remaining atoms.[51] Refinement was performed by the full-matrix least square method based on F^2. Compound $[\mathbf{2}]PF_6$ was successfully refined in the chiral and polar $P2_1$ space group with absolute structure parameter being refined as 0.41(4), which allows no conclusions to be made about the correct direction of the polar axis. Polar structures are unusual for crystals composed of nonchiral cations and anions as in compound $[\mathbf{2}]^+$. In this case, chirality may arise from the different frozen conformers arising from the diphosphane arrangements

and this is reflected in the high thermal parameters of the ethylene groups of these ligands. Because of this, the C(9)–C(10) bond distance of one ethylene bridge was constrained at a fixed value during the refinement.

All atoms in the cluster except the carbon of the diphosphane ligand were refined anisotropically. The structure contains one PF_6^- anion per asymmetric unit and only the phosphorus atom P(10) in the anion was refined anisotropically. The geometry of this anion was refined as rigid group. The positions of all hydrogen atoms were generated geometrically, assigned isotropic thermal parameters and allowed to ride on their respective parent carbon atoms.

Crystal data for [2]PF_6. Empirical formula: $C_{14}H_{35}F_6O_2P_5Se_4W_2$; $M = 1187.81$, crystal system: monoclinic, space group $P2_1$; unit cell dimensions: $a = 8.446(5)$, $b = 12.1795(7)$, $c = 14.728(8)$ Å, $\beta = 91.892(14)°$; $V = 1590.8(15)$ Å^3; $Z = 2$; $T = 293(2)$ K; $\mu = 12.100$ mm^{-1}; theta range for data collection: 2.11–25.00°; reflections collected: 7512; independent reflections: 5150 ($R_{int} = 0.1017$); final R indices [$I > 2\sigma(I)$]; $R1 = 0.0803$, $wR2 = 0.1601$; R indices (all data); $R1 = 0.1822$, $wR2 = 0.2051$. Residual electron density: 1.309 and −1.173 e Å^{-3}.

CCDC reference number 616576.

For crystallographic data in CIF or other electronic format see DOI: 10.1039/b611274a

Acknowledgements

The financial support of the Spanish ministerio de Educación y Ciencia and the EU FEDR Program (Grants CTQ2005-09270-C02-01 and BQU2003-04737), Fundació Bancaixa UJI (Project P1.1B2004-19), Junta de Andalucia (Grupo FQM-137), and Generalitat Valenciana (Project ACOMP06/241) is gratefully acknowledged. The authors also thank the Servei D'Instrumentació Cientifica (SCIC) of the University Jaume I and the Servicios Centrales de Ciencia y Tecnologia of the University of Cadiz for providing us with the mass spectrometry, NMR and X-ray facilities.

References

1 C. Bergquist, T. Fillebeen, M. M. Morlok and G. Parkin, *J. Am. Chem. Soc.*, 2003, **125**, 6189.
2 X.-H. Yamamoto, J.-F. Han and J.-F. Ma, *Angew. Chem., Int. Ed.*, 2000, **39**, 1965.
3 A. Mori, Y. Danda, T. Fujii, K. Hirabayashi and K. Osakada, *J. Am. Chem. Soc.*, 2001, **123**, 10774.
4 K. L. Breno and D. R. Tyler, *Organometallics*, 2001, **20**, 3864.
5 J. R. Fulton, A. W. Holland, D. J. Fox and R. G. Bergman, *Acc. Chem. Res.*, 2002, **35**, 44.
6 J. W. Gilje and H. W. Roesky, *Chem. Rev.*, 1994, **94**, 895.
7 L. Cuesta, D. C. Gerbino, E. Hevia, D. Morales, M. E. Navarro-Clemente, J. Perez, L. Riera, V. Riera, D. Miguel, I. del Rio and S. Garcia-Granda, *Chem. Eur. J.*, 2004, **10**, 1765.
8 S. S. Yarovoi, Y. V. Mironov, D. Y. Naumov, Y. V. Gatilov, S. G. Kozlova, S.-J. Kim and V. E. Fedorov, *Eur. J. Inorg. Chem.*, 2005, 3945.
9 P. R. Robinson, E. O. Schlemper and R. K. Murmann, *Inorg. Chem.*, 1975, **14**, 2035.
10 J. C. Fettinger, H. B. Kraatz, R. Poli and E. A. Quadrelli, *Chem. Commun.*, 1997, 889.
11 D. Morales, M. E. N. Clemente, J. Perez, L. Riera, V. Riera and D. Miguel, *Organometallics*, 2002, **21**, 4934.
12 T. Waters, R. A. J. O'Hair and A. G. Wedd, *J. Am. Chem. Soc.*, 2003, **125**, 3384.
13 T. Waters, R. A. J. O'Hair and A. G. Wedd, *Inorg. Chem.*, 2005, **44**, 3356.
14 T. Waters, R. A. J. O'Hair and A. G. Wedd, *Int. J. Mass Spectrom.*, 2003, **228**, 599.
15 E. Collange, J. A. Garcia and R. Poli, *New J. Chem.*, 2002, **26**, 1249.
16 J. Gun, A. Modestov, O. Lev, D. Saurenz, M. A. Vorotynstev and R. Poli, *Eur. J. Inorg. Chem.*, 2003, 482.
17 J. Gun, A. Modestov, O. Lev and R. Poli, *Eur. J. Inorg. Chem.*, **2003**, 2264.
18 M. G. Basallote, F. Estevan, M. Feliz, M. J. Fernandez-Trujillo, D. A. Hoyos, R. Llusar, S. Uriel and C. Vicent, *Dalton Trans.*, 2004, 530.
19 M. G. Basallote, M. Feliz, M. J. Fernandez-Trujillo, R. Llusar, V. S. Safont and S. Uriel, *Chem. Eur. J.*, 2004, **10**, 1463.
20 R. Bakhtiar and C. E. C. A. Hop, *J. Phys. Org. Chem.*, 1999, **12**, 511.
21 L. S. Santos, L. Knaack and J. O. Metzger, *Int. J. Mass Spectrom.*, 2005, **246**, 84.
22 L. A. Dakin, P. C. Ong, J. S. Panek, R. J. Staples and P. Stravropoulos, *Organometallics*, 2000, **19**, 2896.
23 F. Dallavale and M. Tegoni, *Polyhedron*, 2001, **20**, 2697.
24 A. R. S. Ross and S. L. Luettgen, *J. Am. Soc. Mass Spectrom.*, 2005, **16**, 1536.
25 J. Dai, G.-Q. Bian, X. Wang, Q.-F. Xu, M.-Y. Zhou, M. Munakata, M. Maekawa, M.-H. Tong, Z.-R. Sun and H.-P. Zeng, *J. Am. Chem. Soc.*, 2000, **122**, 11007.
26 M. Sokolov, P. Esparza, R. Hernandez-Molina, J. G. Platas, A. Mederos, J. A. Gavin, R. Llusar and C. Vicent, *Inorg. Chem.*, 2005, **44**, 1132.
27 R. Llusar, S. Triguero, C. Vicent, M. N. Sokolov, B. Domercq and M. Fourmigue, *Inorg. Chem.*, 2005, **44**, 8937.
28 R. W. M. Wardle, C.-N. Chau and J. A. Ibers, *J. Am. Chem. Soc.*, 1987, **109**, 1859.
29 R. W. M. Wardle, S. Bhaduri, C.-N. Chau and J. A. Ibers, *Inorg. Chem.*, 1988, **27**, 1747.
30 Y.-J. Lu, M. A. Ansari and J. A. Ibers, *Inorg. Chem.*, 1989, **28**, 4049.
31 L. Xu, J. Huang, D. Yan and Q. Zhang, *Inorg. Chem.*, 1996, **35**, 1389.
32 J. E. Drake, A. G. Mislankar and R. Ratnani, *Inorg. Chem.*, 1996, **35**, 2665.
33 N. C. Howlader, G. P. J. Haight, T. W. Hambley, M. R. Snow and G. A. Lawrance, *Inorg. Chem.*, 1984, **23**, 1811.
34 R. Dessapt, C. Simmonet-Jegat, J. Marrot and F. Secheresse, *Inorg. Chem.*, 2001, **40**, 4072.
35 R. Dessapt, C. Simmonet-Jegat, A. Mallard, H. Lavanant, J. Marrot and F. Secheresse, *Inorg. Chem.*, 2003, **42**, 6424.
36 A. Seigneurin, T. Makani, D. J. Jones and J. Rozière, *J. Chem. Soc., Dalton Trans.*, 1987, 1878.
37 *Cambridge Crystallographic Data Center v. 5.26*, 2006 (last updated November 2005).
38 A. G. Algarra, M. G. Basallote, M. Feliz, M. J. Fernandez-Trujillo, R. Llusar and V. S. Safont, *Chem. Eur. J.*, 2006, **12**, 1413.
39 Y. G. Yao, H. Akashi, G. Sakane and T. Shibahara, *Inorg. Chem.*, 1995, **34**, 42.
40 Y. H. Tang, Y. Y. Qin, L. Wu, Z. J. Li, Y. Kang and Y. G. Yao, *Polyhedron*, 2001, **20**, 2911.
41 Y. Y. Qin, Y. H. Tang, Y. Kang, Z. J. Li, R. F. Hu, J. K. Cheng, Y. H. Wen and Y. Yao, *J. Mol. Struct.*, 2004, **707**, 235.
42 E. Guillamon, R. Llusar, O. Pozo and C. Vicent, *Int. J. Mass Spectrom.*, 2006, **254**, 28.
43 K. Izutsu, *Acid–Base Dissociation Constants in Bipolar Aprotic Solvents*, Blackwell Scientific Publications, Oxford, 1990.
44 R. G. Wilkins, *Kinetics and Mechanism of Reactions of Transition Metal Complexes*, VCH, Weinheim, 2nd edn, 1991.
45 Q. M. Nasreldin, A. Olatunji, P. W. Dimmock and A. G. Sykes, *J. Chem. Soc., Dalton Trans.*, 1990, 1765.
46 D. M. Saysell, V. P. Fedin, G. J. Lamprecht, M. N. Sokolov and A. G. Sykes, *Inorg. Chem.*, 1997, **36**, 2982.
47 R. Hernandez-Molina and A. G. Sykes, *J. Chem. Soc., Dalton Trans.*, 1999, 3137.
48 R. A. Binstead, B. Jung and A. D. Zuberbühler, *SPECFIT/32*, Spectrum Software Associates, Chapel Hill, 2000.
49 *SAINT 5.0*, Bruker Analytical X-Ray Systems, Madison, WI, 2001.
50 G. M. Sheldrick, *SADABS empirical absorption correction program*, University of Göttingen, 2001.
51 G. M. Sheldrick, *SHELXTL 5.1*, Bruker Analytical X-Ray Systems, Madison, WI, 1997.